ATP Production by Oxidative Metabolism and Blood Flow Augmentation by Non-oxidative Glycolysis in Activated Human Visual Cortex

A-L. Lin[1], J-H. Gao[2], T. Q. Duong[1], and P. T. Fox[1]
[1]Research Imaging Institute, University of Texas Health Science Center at San Antonio, San Antonio, TX, United States, [2]Brain Research Imaging Center, University of Chicago, Chicago, IL, United States

Introduction: Increase in cerebral blood flow (CBF) and energy demands (ATP production; J_{ATP}) are accompanied with neuronal activation. However, whether they are mediated by oxidative or non-oxidative metabolic pathway remained a subject of study (1, 2). The purpose of the present study was to use concurrent fMRI and ^{1}H MRS methods to re-visit the issues. Specifically, we sought: 1) to quantify the relative contributions of oxidative and non-oxidative metabolic pathways in meeting the increased energy demands (J_{ATP}) of task-induced neuronal activation; and, 2) to determine whether task-induced CBF augmentation was regulated by oxidative or non-oxidative metabolic pathways. A multi-rate visual stimulation paradigm was used in the study.

Material and Methods: Twelve healthy volunteers (aged 22-38) participated in this study. A black-white checkerboard was used. Rates of 4Hz, 8 Hz and 16Hz were given in a radon order interleaved with resting state (4 min each). Experiments were performed on a 3T Siemens Trio MRI scanner (Siemens, Erlangen, Germany) with simultaneous VASO, ASL, and BOLD measurement using a pulse sequence described previously (3). A standard Transmit/Receive head coil was used. A single oblique axial slice (6 mm in thickness) that included the primary visual cortex was chosen. Images were acquired with a FOV= 26 cm, matrix size = 64 x 64, TE for VASO/ASL/BOLD = 9.4/11.6/28.1 ms, TR=2000 ms, TI_1/ TI_2= 610/1200 ms and inversion slab thickness= 100 mm. Data were processed and analyzed using MATLAB 7 (Math Works, Natick, MA). Student's *t* tests were used to compare "baseline" and each frequency "stimulus" signals. The threshold was set to t = 3.0 ($P < 0.005$). Only those common activation areas that passed the statistically significant threshold for all the VASO, ASL, and BOLD functional maps across all three visual stimulation frequencies were utilized for calculating the average values of the %ΔCBV, %ΔCBF, and %ΔBOLD, respectively. The three functional quantities were then used to calculate the $\%\Delta CMRO_2$ with the following equation (4, 5):

$$\%\Delta CMRO_2 = \left(1 - \frac{(\%\Delta BOLD)}{M}\right)^{\frac{1}{\beta}} \cdot (1 + \%\Delta CBV)^{-\frac{1}{\beta}} \cdot (1 + \%\Delta CBF) - 1$$

Following the fMRI study, the *in vivo* ^{1}H NMR spectra were obtained using the PRESS localization approach with TR/TE=2000/30 ms. The spectral width (FWHM) was 24 Hz. A voxel of interest (VOI) was positioned within the primary visual cortex (V1) centered on the calcarine fissure. The VOI was 25×21×30 mm^3 for a volume of 15.8 cc. Visual stimulation was performed as described above. The paradigm consisted of 4-min (120 averages) visual stimulus at each frequency alternating with 4-min baseline condition. Data (FIDs) for every 120 averages were summed in blocks and further processed using Nuts NMR data processing software (Acorn NMR Inc., Livermore, CA, USA), including a Fourier transform, frequency correction, phase correction and baseline correction of the FID. Lactate concentrations during resting and activation states were determined from the ratio of intergraded intensities centered at 1.33 ppm and the *N*-acetylaspartate (NAA) resonance at 2.02 ppm. Relative lactate concentration (Δ[Lac](%)) was determined by comparing the activation states to the resting state. ΔJ_{Lac}(%) was determined with Δ[Lac] divided by intergraded time period (4 min). JATP can then be determined by the following equation (derived from equations in ref (6)):

$$J_{ATP(a)} = J_{Lac(r)} \times (1 + \%\Delta J_{Lac}) + \frac{19}{3} CMRO_{2(r)} \times (1 + \%\Delta CMRO_2)$$

where "r" and "a"denote resting activation state, respectively. $CMRO_{2(r)}$ and $J_{Lac(r)}$ were assumed 0.42 and 0.27μmol/g/min, respectively (2,6).

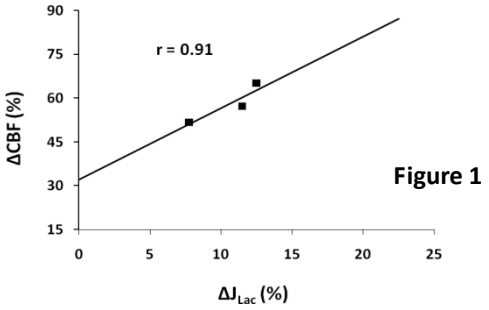

Figure 1

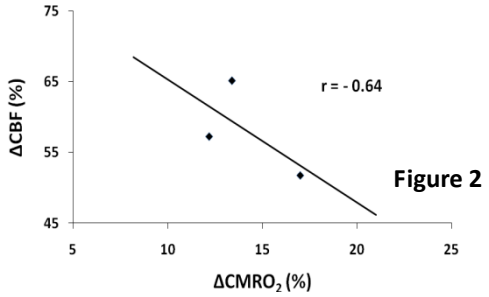

Figure 2

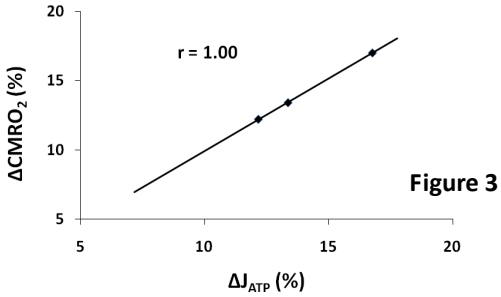

Figure 3

Results and Discussion: As demonstrated in Table 1, both %ΔCBF and %Δ[Lac] (~ $\%\Delta J_{Lac}$) reached their maximum at 8 Hz. As a result, %ΔCBF was highly correlated with $\%\Delta J_{Lac}$ (r = 0.91, P < 0.001) (Figure 1). In contrast, $\%\Delta CMRO_2$ reached a maximum at 4 Hz with no significant difference across the three frequencies (P > 0.5). Non-linear coupling and a negative correlation was found between %ΔCBF and $\%\Delta CMRO_2$ (r = -0.64, Figure 2). The observed relationship between %ΔCBF and $\%\Delta CMRO_2$ in this work are consistent well with recent fMRI and PET findings (4,5,7). $J_{ATP(a)}$ was predominately due to oxidative metabolism (~ 98%) at 4 Hz, which represents the lowest $\%\Delta J_{Lac}$ and highest $\%\Delta CMRO_2$ of the three stimuli. Interestingly, a similar result of ~98% oxidative contribution in total to $J_{ATP(a)}$ was also seen at 8 and 16 Hz, even though %Δ[Lac] rose while $\%\Delta CMRO_2$ declined. $\%\Delta J_{ATP}$ is thus shown to tightly correlate with $\%\Delta CMRO_2$ (r = 1.00, P < 0.001, Figure 3). These results indicate that: 1) the energy demands of task-induced brain activations are small (~15%) relative to the hyperemic response (~60%); 2) that energy demands are met through oxidative metabolism; and, 3) that the CBF response is mediated by glucose consumption, here indexed by lactate production, rather than oxygen demand.

	ΔBOLD(%)	ΔCBV(%)	ΔCBF(%)	$\Delta CMRO_2$(%)	Δ[Lac](%)	ΔJ_{Lac}(%)	ΔJ_{ATP} (%) (aerobic)	ΔJ_{ATP} (%) (anaerobic)
4Hz	1.8 ± 0.4	19.0 ± 4.6	51.7 ± 7.8	17.0 ± 3.3	31.3 ± 4.4	7.8 ± 1.1	97.8 ± 2.0	2.2 ± 2.0
8Hz	2.5 ± 0.2	28.5 ± 3.8	65.1 ± 5.9	13.4 ± 4.0	50.0 ± 5.7	12.5 ± 1.5	97.6 ± 2.1	2.4 ± 2.1
16Hz	2.3 ± 0.3	24.8 ± 5.1	57.2 ± 6.2	12.2 ± 4.1	46.1 ± 4.7	11.5 ± 1.2	97.6 ± 2.1	2.4 ± 2.1

Table 1 Variables obtained with fMRI and ^{1}H NMR spectroscopy for each of the visual stimulation rates

References: (1) Hoge et al., 1999 MRM 42:849–863; (2) Fox et al., 1988 Science 241:462-464; (3) Yang et al., 2004, MRM 52:1407-1417;(4) Lin et al., 2008 MRM 60:380–389; (5) Lin et al., 2009 Neuroimage 44:16–22; (6) Gjedde 1997 in Cerebrovascular Disease 23-40; (7) Vafaee and Gjedde, 2000, JCBFM 20:747-754.